

Project Title: Transport properties of self-propelled micro-swimmers

Name: Dr. Franco Nori (team leader)

Dr. Pulak Kumar Ghosh

Laboratory at RIKEN: Quantum Condensed Matter Research Group, Center for Emergent Matter Science

I. Background and purpose:

Artificial microswimmers are active particles capable of autonomous propulsion[1]. A common class of such micromotors are the so-called Janus particles (JP), mostly spherical objects with two differently-coated hemispheres, or faces. Due to the different functionalization of their faces, JP's harvest kinetic energy from their environment, by generating local (electric, thermal, or chemical gradients in the suspension medium (self-phoresis).

Among the most promising technological applications of artificial microswimmers is their usage as motors [1-2], whereby they couple to a cargo, represented by a passive particle (PP), and tow it from a docking to an end station, often along an assigned track engraved on a 2D micro-fluidic chip. In such configuration, tower and cargo form a dimer with one active head, the JP, and a swerving tail, the PP. The diffusion of such a dimer is fuelled by the self-phoretic force acting upon the JP, while both monomers are subjected to a viscous drag.

The self-phoretic mechanism activated by the JP generates a short-range hydrodynamic backflow in the viscous suspension fluid, which may result in an additional pair interaction between the monomers. However, at low Reynolds numbers, as the active swimmer tows its cargo, it generates a laminar flow that tends to align the dimer's axis parallel to the propulsion force, with the PP trailing the JP. It is known that the dipolar hydrodynamic interactions associated with the swimmer's propulsion mechanism decay faster with the distance than the perturbation due to the laminar flow caused by its steady translation. Therefore, the average

tower-cargo distance can be conveniently chosen, so as to ignore the short-range hydrodynamic interaction between them with respect to the long-range hydrodynamic effects on their viscous drag. As we propose to utilize active microswimmers to transport cargos in a controllable manner, it becomes important to study the diffusive dynamics of an active dimer in the laminar flow maintained, say, in a micro-fluidic device. The hydrodynamics of active systems, including both single and clustering microswimmers, possibly in confined geometries, is an extensive topic. In this work, we limit ourselves to considering the case of an elastic dimer suspended in a highly viscous fluid coned between two parallel plates. The two plates may slide in opposite directions with equal speed, thus generating the simplest and more tractable example of laminar shear flow in the fluid (Couette flow). To avoid unnecessary complications, we assume that tower and cargo have equal mass and viscous constant. Therefore, here the two monomers can be regarded as identical, except that the JP is subject to a fluctuating force of constant modulus, which represents the pull from the self-propulsion mechanism. When moving, each particle generates a laminar flow that affects the diffusion of its partner and, eventually, the diffusivity of the entire dimer.

We perform extensive Brownian dynamics simulations of such a bound system in 3D and focused on the hydrodynamic corrections to the dimer's diffusion constant. In a Couette flow, corrections due to long-range hydrodynamic interactions become prominent in the dynamical

regime when the speeds of the self-propelling dimer and the sliding plates are comparable.

Model

The overdamped Brownian dynamics of a pair of identical interacting particles of mass m , radius a , and viscous constant, suspended in a fluid at rest with temperature T , has been numerically simulated by Ermak and McCammon [3]. Upon expressing time in units of $1/\gamma$ and all lengths in units of p (kT/γ^2m)^{1/2}, their integration algorithm reads (in Einstein summation convention)

$$r_i(t + \Delta t) = r_i(t) + v_i \Delta t + \frac{\partial}{\partial r_j} D_{ij} \Delta t + \frac{D_{ij}}{D_0} f_j + \eta_i(\Delta t) \dots (1)$$

where the repeated indices i and j run over the particle coordinates, Δt integration step, and η_i are zero-mean valued, delta-correlated Gaussian noises with (co)variance $\langle \eta_i(\Delta t) \eta_j(\Delta t) \rangle = 2D_{ij} \Delta t$. The drag velocities, v_i , are the components of the unperturbed shear flow in the Couette cell at the point occupied by the center of the particles. The force f_j is composed of two terms: (1) An internal force due to the elastic pair potential, $U = k(r_{ij}-l)^2$, (2) The self propulsion, p , acting on the JP. Its modulus, p , is fixed, while its orientation fluctuates in time with law,

$$\dot{\hat{p}} = \hat{p} \times \xi(t) \dots (2)$$

where \hat{p} is the relevant unit vector and the three Cartesian components of the Gaussian noise $\xi(t)$ are independent, zero-mean valued, and delta-correlated with variance $\langle \xi_i(\Delta t) \xi_j(\Delta t) \rangle = 2D_r \Delta t$. The quantity D_r controls the time decay of the p autocorrelation function, $\langle p_i(t) p_i(0) \rangle = (p^2/3) \exp[-2D_r |t|]$, and D_r is referred to as the JP rotational constant. Moreover, the confining action of the sliding plates in a Couette cell has been mimicked by introducing an additional force perpendicular to the plates (see Fig.1). Accordingly, the shear flow across the cell assumes the simple linear expression, $v(y)/v_s = 2y/L$, while the remaining z coordinate can be ignored. Due to symmetry considerations, the net drift velocity of the dimer is identically zero.

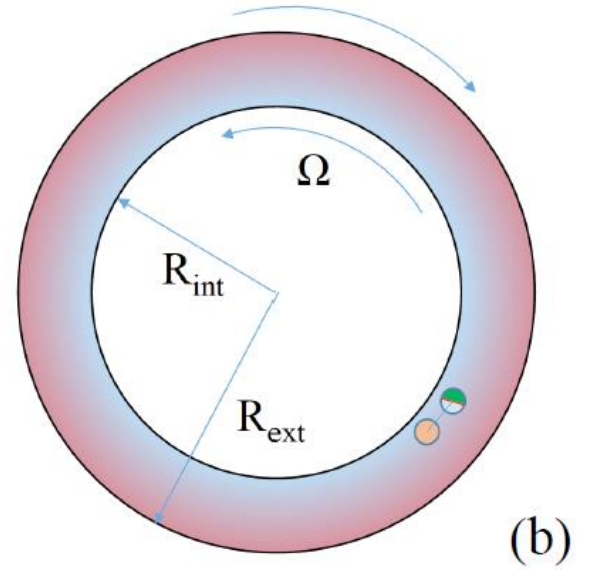
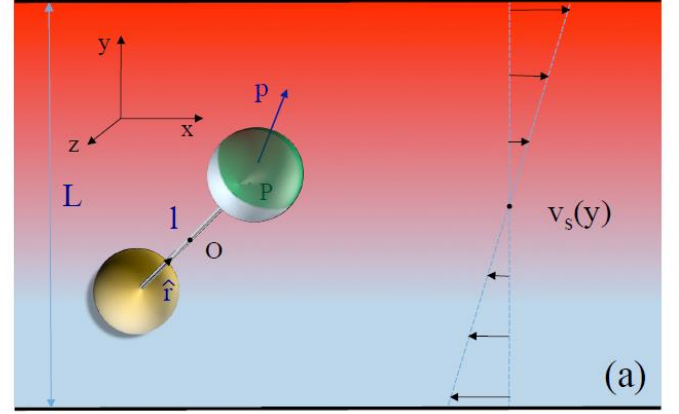


FIG. 1: (Color online) Active dimer self-propulsion mechanism: (a) active elastic dimer model. O and P are respectively the center of mass and the center of force of the dimer formed by an active and a passive particle of equal shape, bound together by an elastic string. p represents the instantaneous self-propulsion force and \hat{l} the dimer's length vector oriented from the passive to the active particle. (b) Couette cell. A shear flow is generated between two concentric rings of radius R_{int} and R_{ext} , with $R_{\text{ext}} - R_{\text{int}} = L$, rotating with opposite angular frequency .

III. Methods

Our studies are based on the numerical simulation of Langevin equations (1) and (2) with Oseen Diffusion tensor [3] D_{ij} . An exact analytical solution of the Langevin equation is impossible. One can overcome

this difficulty by numerically solving the Langevin equations. We used Milstein algorithm [4] to numerically solve the equation (1). Appropriate boundary conditions have been used to account for the shape of the Janus particles and the structure of the confining walls. To calculate diffusion tensor we exploit the method described in the ref[3].

We calculate diffusivity, which is quantified by the diffusion constant,

$$D_d = \lim_{t \rightarrow \infty} (\langle x^2 \rangle - \langle x \rangle^2) / 2t$$

where x is the coordinate of the JP particle and the stochastic average, $\langle \rangle$, is taken over at least 2×10^3 trajectories. Indeed, for exceedingly long observation times, in our runs $t > 10^9 \Delta t$ or larger, the dimer length becomes negligible with respect to the dimer displacement, and so are the initial condition transients.

II. Results and conclusions

Diffusion of passive dimer in a Couette flow:

We first study diffusive properties of a simple system composed by two identical passive particles of radius a , bound by the elastic potential under action of Couette flow field. Our simulation results show that diffusivity comprise of two components that accounts for normal thermal diffusion of the dimer and flow induced diffusivity. At very low flow field strength diffusivity is dictated by the thermal motion and independent of v_s . With increasing strength of flow field, diffusivity gradually starts growing quadratically with v_s . The simulations results can be explained with some simple phenomenological arguments. Moreover, our simulation data recover the results of rigid dimer when the bonding potential between the monomers are very strong. In this limit diffusivity grows linearly with size of the monomer due hydrodynamic correction.

To better understand hydrodynamic correction in the diffusivity, we also calculate the ratio, $D/D(0)$, where $D(0)$ denotes the numerically simulated diffusion constant for the same parameters as D ,

except for $a = 0$. This quantity is thus a measure of the hydrodynamic corrections to the diffusion constant of a dimer under general shear and activation conditions. At small v_s the ratio increases with increasing size of the monomers where as at large v_s it decreases. Most remarkably, the hydrodynamic corrections to D eventually vanish for extremely large shear flows, as implied by the asymptotic limit $D/D(0) \rightarrow 1$, for v_s tends to infinity. We explain this property recalling that, during their roto-translational motion, two bound monomers maintained at a finite distance are, in general, subject to different local shear flows, which causes an additional strain on the dimer's bond. One thus expects the ratio a/l to diminish with raising v_s , which leads to a progressive suppression of the hydrodynamic effect.

Diffusion of active dimer in Couette flow:

The diffusion constant of an active swimmer, consists of a thermal, and a self-propulsion term, the latter being typically much larger than the former. Hydrodynamic corrections to these two diffusion terms must be treated separately. Moreover, when propelling itself in a shear flow, an elastic dimer is subject to hydrodynamic effects that result from the non trivial interplay of shear and activation. To have closer look on the essential features, we analyzed our numerical results for an active dimer in a suspension fluid at rest and the more complicated case of an active dimer in a Couette flow separately.

(a) Diffusion of active dimer in absence of flow field--

The data sets displayed in Fig2(a) clearly show a transition between two diffusive regimes, which we agree to term thermal and active, respectively. Indeed, at low p , the diffusion constant is insensitive to p and dominated by thermal fluctuations, while at large p it grows quadratically with p . The dependence of D on the self-propulsion force is qualitatively well reproduced by a sequence of substitutions $D_d \rightarrow D_0/2$, $D_s \rightarrow \frac{v_0^2}{6Dr}$, $D_0 \rightarrow D_0(1 +$

a/l , $v_0 \rightarrow v_0(1 + a/l)$ and $v_0 \rightarrow p$. The final expression,

$$D = D_d(1 + a/l) + \frac{p^2}{24D_r}(1 + a/l)^2 \quad \dots(3)$$

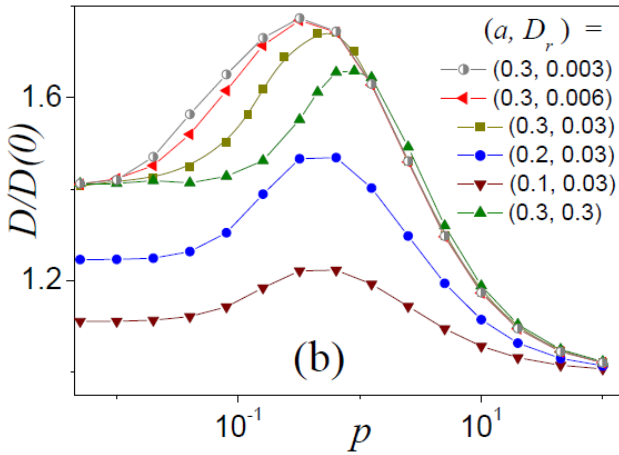
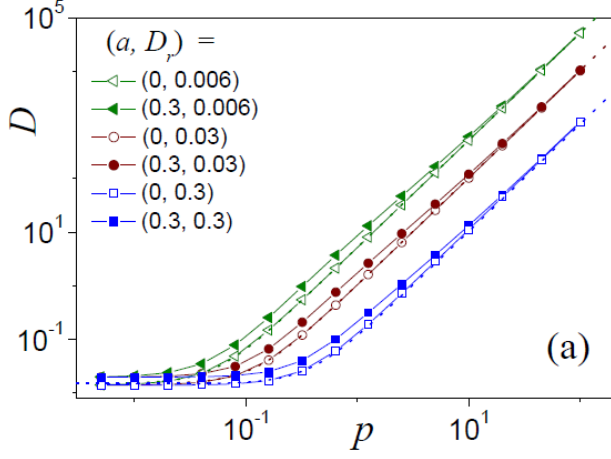


Fig2: Active dimer diffusion at zero shear flow: (a) D vs. p for different values of the monomer radius, a , and the angular diffusion, D_r . The dashed curves are the analytical prediction of Eq. (3) with $a = 0$; (b) $D/D(0)$ vs. p for different a and D_r . $D(0)$ denotes the particle's diffusion in the absence of hydrodynamic corrections, $a = 0$. Other simulation parameters are: $k = 1$, $l = 1$, $L = 10$, $v_s = 0$, and $D_0 = D_r = 0.03$.

It suggests a crossover between thermal and active diffusion which is in fair agreement with our numerical data. In view of Eq. (3), one expects that in the active diffusion regime, the ratio $D/D(0)$ is expected to coincide asymptotically with the square

of the same ratio at $p = 0$ (thermal regime), namely, $D/D(0) = (1+a/l)$ for $p = 0$, and $D/D(0) \rightarrow (1+a/l)^2$ for $p \rightarrow \infty$.

When increasing p larger than the crossover value of the self-propulsion p_c , the numerical data seem to support our expectations also for the rather large ratios a/l reported in Fig. 2(b). However, on further increasing p , this asymptotic prediction fails. A more detailed analysis of our numerical data clearly shows that all ratios $D/D(0)$ eventually decay to 1 like $D/D(0) - 1$ proportional to a/p . This produces the bell-shaped profile of the curves $D/D(0)$ versus p .

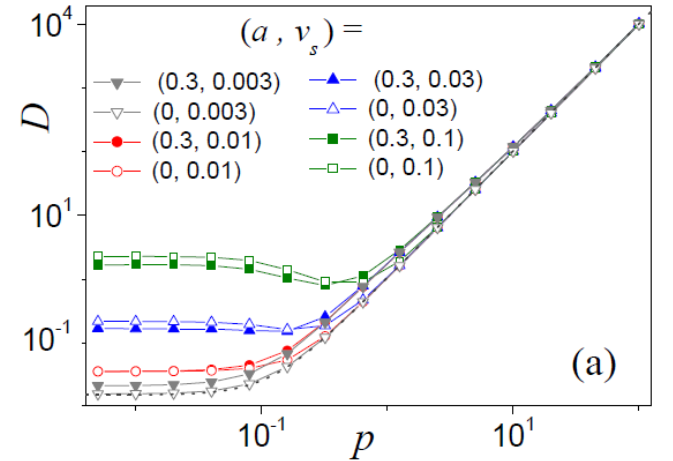
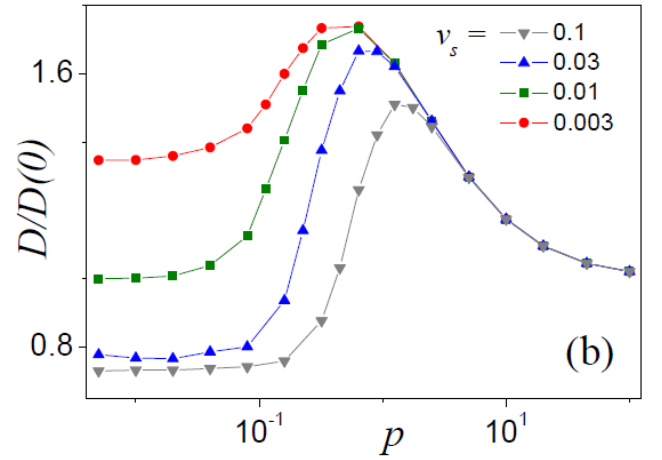


Fig3: Active dimer diffusion in a Couette cell with different plate sliding speed, v_s : (a) D vs. p for $a = 0$ and 0.3. The dashed curve is the analytical prediction of Eq. (3) with $a = 0$; (b) $D=D(0)$ vs. p for $a = 0.3$ and different v_s . $D(0)$ denotes the particle's diffusion in the absence of hydrodynamic corrections, $a = 0$. Other simulation parameters are: $k = 1$, $l = 1$, $L = 10$, and $D_0 = D_r = 0.03$.

(b) *Diffusion of active dimer in the presence of flow filed* -- Simulation data for the diffusion constant of an active dimer self-propelling in a Couette cell with plate sliding speed v_s are plotted in Fig. 3. In Fig. 3(a) we illustrate the dependence of D on the modulus of the self-propulsion force, p , for different values of v_s . At low p , as expected, one recovers the diffusion constant of the corresponding passive dimer. At large p , instead, D grows quadratically with p , as discussed in the previous section in the absence of shear flow, $v_s = 0$. The crossover between shear and active diffusion occurs for a value of the force, p_s , which can be estimated by comparing the relevant (approximate) expressions for D at $p = 0$, and $v_s = 0$. For large shear flows, $v_s > v_s^c$, one immediately sees that $p_c = \sqrt{D_r D_0} v_s L$, in good agreement with the data in Fig. 3(a).

On a closer inspection, one also notices that, for higher shear flows, in Fig. 3(a) the low p branch of the curves $D(p)$ develop a negative curvature. This is a consequence of the fact that (for $p = 0$ and $v_s > v_s^c$) the diffusion constant is approximately proportional to the mean first passage time, across the Couette cell. An explicit calculation shows that relaxation time is quite sensitive to the active component of the dimer's Brownian motion [37] and, more precisely, decreases with increasing p . This causes the small dips in the diffusion curves observed for the highest v_s plotted of Fig. 3(a). These two distinct diffusion regimes are clearly visible also in Fig. 3(b), where, our data for the ratio $D/D(0)$, at $p = 0$, start with the corresponding value for $a = 0.3$ of passive dimer and, for p tends to infinity, decay asymptotically to 1. More interesting is the intermediate p range, where the hydrodynamic effect on the dimer diffusion is magnified by the interplay between shear and activation. At low v_s , we recover the bell-shaped curves already reported in Fig. 2(b) for zero shear. On raising the self-propulsion force for v_s larger but close to v_s^c , the ratio $D/D(0)$ jumps from below 1 up to a maximum of the order of 2. The

relative correction to the constant D due to the hydrodynamic interactions, thus proves to be quite large. The maxima of the curves $D/D(0)$ versus p are not higher than the maximum obtained in the absence of shear flow, i.e., for $v_s = 0$, which, based on Eq. xx), we know to be centered at $p \sim p_s$ and of the order of $(1 + a/l)^2$. Note, however, that the validity of Eq. (3) is restricted by the condition $p \gg v_s$. Accordingly, as one increases v_s , the ratio $D/D(0)$ becomes suppressed for $p < v_s$ and, consequently, its maximum lowered and shifted to higher p .

IV. Future Plan

The following items are the main objectives for the next fiscal year which are the important and essential extension of our previous works:

(a) Single file diffusion of self-propelled Janus particles:

The single file dynamics refer to motion of the many particles in a narrow channel where particles cannot cross each other. Such type of file dynamics arise in many situations in nano-technology and biological sciences. For an example, diffusion of ions or large organic molecules in narrow biological channels. The most conspicuous feature of the diffusion of particles as a single file is that the mean square displacement (MSD) is proportional to the square root of time in some time domains and its probability density function is Gaussian in position with a variance MSD. The single file dynamics of the normal Brownian particles are well studied and provide reasonable explanation to some phenomena occurs in biological cells.

Keeping mind all the recent advances in this direction, we want to explore single file dynamics of active particles and also for active-passive mixture. To be specific we want study file dynamics for a system of self-propelled Janus particles (JP). As this type of particles can propel themselves by harvesting kinetic energy from an active environment, they have a different type of diffusion mechanism. In the absence of any external force field,

Usage Report for Fiscal Year 2016

the motion of a self-propelled JP is directed parallel to the self-phoretic force. Gradient fluctuations or collisions with boundaries or the intrinsic rotational diffusion result in a random change of the direction of self-propulsion. Thus, self-propelled JPs exhibit time correlated active Brownian motions. We expect the system of Janus particles or active-passive mixture may exhibit a considerably different file dynamics from normal Brownian particles. Moreover, understanding single file dynamics of JPs is potentially important for targeted drug delivery where they need to pass through a narrow path.

(b) Effusion of active passive particle mixture:

In the next fiscal year we also want to explore dynamics of interacting active-passive mixtures to understand how kinetic energy of active particles can be exploited to speed up slowly moving passive particles. This type of study may have many direct applications. Particularly, fast diffusing Janus particles can be used to clean biological channels clogged by sluggish particles. Also, in many situation it would be desirable to improve distribution of particle velocity so that weak particles can play their role to function some biological process. For example, if we have some percent of "weak" particles (e.g., weak sperm cells that are not able to reach/penetrate the egg) with initial distribution, and then, by adding other active particles, we can "help" those weak cells to move faster and thus do their job.

Here we want to calculate two quantifiers, effusion rate and velocity distribution, to understand the control mechanism of speeding up weak particles by adding Janus particles as an external aid.

Method

To address the issues mentioned above following model and method will be used.

Model: In order to avoid unessential complications, we will restrict ourselves to the case of 2D channels and finite sized artificial micro-swimmers of the Janus particle type. In some cases, it is quite straightforward to extend conclusions of 2D

problems to three-dimensional ones. A Janus particle gets a continuous push from the suspension fluid, which amounts to a rotating self-propulsion force F with constant modulus F_0 . Additionally, the self-propulsion direction varies randomly with time due to the rotational diffusion. The bulk dynamics of a self-propelled Janus particles can be described by the following set of equations under the combined action of thermal noise and orientation fluctuations.

$$\dot{x} = -\gamma\dot{x} + F_0 \cos\theta + \sqrt{\gamma kT} \xi_x(t)$$

$$\dot{y} = -\gamma\dot{y} + F_0 \sin\theta + \sqrt{\gamma kT} \xi_y(t)$$

$$\dot{\theta} = \xi_\theta + \Omega$$

where (x, y) denote the position of the particle center of mass. $\xi_x(t)$, $\xi_y(t)$ and $\xi_\theta(t)$ are zero mean, delta-correlated Gaussian noises. γ is the damping constant depends on the particle size and medium viscosity. k and T are Boltzmann constant and temperature, respectively. The effective dynamics of JPs becomes more complicated in the presence of hydrodynamics interactions and confinements.

Beside a few ideal cases, an exact analytical solution of the Langevin equation is impossible. One can overcome this difficulty by numerically solving the Langevin equations. We will numerically solve the Langevin equations using a Milstein algorithm [4] with appropriate boundary conditions to account for the shape of the Janus particles and the structure of the confining walls. In addition to the thermal noise and self-propulsion, remaining physical force terms arise either due to hydrodynamic interactions or due to intrinsic and externally applied forces have been incorporated into the Langevin description.

Currently, I have a "Quick Use" user account and I would like to get extension of computation facilities for next usage term (up to 31st March 2018) under the same user category.

References:

- [1] F. Schweitzer, *Brownian Agents and Active Particles* (Springer, Berlin, 2003); S. Ramaswamy, *Annu. Rev. Condens. Matter Phys.* **1**, 323 (2010); P.

Usage Report for Fiscal Year 2016

- Romanczuk *et al.*, Eur. Phys. J. Spec. Top. **202**, 1 (2012); T. Vicsek *et al.*, Phys. Rep. **517**, 71 (2012).
- [2] P. K. Ghosh, V. R. Misko, F. Marchesoni, and F. Nori, Phys. Rev. Lett. **110**, 268301 (2013).
- [3] D. L. Ermak and J. A. McCammon, J. Chem. Phys. **69**, 1352 (1978).
- [4] P. Kloeden *et al.*, Numerical Solutions of Stochastic Differential Equations (Springer, Berlin, 1999).

Usage Report for Fiscal Year 2016

Fiscal Year 2016 List of Publications Resulting from the Use of the supercomputer

[Publication]

1. Communication: Cargo towing by artificial swimmers, Debajyoti Debnath, Pulak K. Ghosh, Yunyun Li, Fabio Marchesoni and Baowen Li, Journal of Chemical Physics 145, 191103 (2016); doi: <http://dx.doi.org/10.1063/1.4967773> (Online publication date: 16th November 2016).

[Proceedings, etc.]

None

[Oral presentation at an international symposium]

None

[Others (Press release, Science lecture for the public)]

None